PROCEEDINGS OF SPIE

Iterative algorithm for layered optical remote sensing reflectance modeling of natural waters with depth-dependent aquatic constituent

Charles R. Bostater
Lisa H. Huddleston
Carrie Semmler
John Mieles

SPIE.

An Iterative Algorithm for Layered Optical Remote Sensing Reflectance Modeling of Natural Waters with Depth Dependent Aquatic Constituent Concentrations

Charles R. Bostater, Jr.[*], Lisa Huddleston, Carrie Semmler, John Mieles

Marine Environmental Optics Laboratory & Remote Sensing Center

College of Engineering

Florida Tech

ABSTRACT

This paper describes the radiative transfer of the sun's electromagnetic energy utilizing a solution to the two-flow irradiance equations that generates fast and accurate estimates of light distributions in any layered media, such as water with depth dependent concentrations of water column constituents. The layered model is designed to generate synthetic water surface reflectance signatures and associated synthetic images, in the presence of depth dependent water constituents, various bottom types, and variable water depths. The layered model accounts for specular (collimated) irradiance below the water's surface and utilizes boundary conditions that allow the absorption, backscatter, beam attenuation, and conversion (from specular irradiance to diffuse irradiance) coefficients to vary as a function of depth. In addition, the model allows one to compute the influences of submerged targets, bottom types or unique submerged targets or water column layers with defined by their reflectance signatures or unique absorption and backscatter characteristics. Model simulations are presented to demonstrate the utility of the model for development of remote sensing algorithms for use in coastal and marine water types.

Keywords: Hyperspectral remote sensing, synthetic images, synthetic signatures, modeling, simulation, water surface reflectance, layered media, absorption, backscatter, submerged targets, bottom types, bottom reflectance, water quality, hydrologic optics

1. BACKGROUND

Understanding radiative transfer in layered media is complicated by large temporal and spatial variability in the optical properties of the medium. This complexity necessitates the use of theoretical models both to interpret and extrapolate observational data. A mathematical reflectance model of a water body, which is based on the spectral characteristics of the water body, can connect the factors that cause a particular reflectance signature with the signature itself. However, there are often trade-offs between detailed physics and computational simplicity[1]. The numerical model derived here generates an approximate solution to the integro-differential radiative transfer equation described by Priesendorfer[2] for a layered water column in one spatial dimension:

$$\cos\theta \frac{dL(\theta,\phi,z,\lambda)}{dz} = -c_{tc}(z,\lambda)L(\theta,\phi,z,\lambda) + \int_{\phi=0}^{2\pi}\int_{\theta=0}^{\pi} \beta(\theta',\theta,\phi',\phi,z,\lambda)L(\theta',\phi',z,\lambda)\sin\theta' d\theta' d\phi'$$

$$+ \beta(\theta_s,\theta,\phi_s,\phi,z,\lambda)L_s(\theta_s,\phi_s,z,\lambda), \quad (\text{Wm}^{-3}sr^{-1}) \tag{1}$$

where z=water depth, positive downward, z=0 at the surface (m), $c_{tc}(z)$=total beam attenuation coefficient (m^{-1}), $\beta(\theta',\theta,\phi',\phi,z,\lambda)$ = volume scattering function of diffused radiance (m^{-1} sr^{-1}), $\beta(\theta_s,\theta,\phi_s,\phi,z,\lambda)$ =volume scattering

---

[*] Dr. Charles R. Bostater, Jr. bostater@probe.ocn.fit.edu; ph: 321 258-9134; fax: 321 773-0980; http://www.ocn.fit.edu; Center for Remote Sensing, Marine and Environmental Optics Laboratory, 150 West University Blvd., Melbourne, FL, USA 32901

function of collimated radiance (m^{-1} sr^{-1}), $L(\theta_s,\phi_s,z,\lambda)$ =collimated radiance (W m^{-2} sr^{-1}), θ_s, ϕ_s =solar zenith angle (θ_s) and solar azimuth angle (ϕ_s) (radians), λ =wavelength of light.

Solutions to the radiative transfer equation (RTE) require simplification of the RTE in order to develop models that generate fast and accurate estimates of light distributions in any layered media, keeping input parameters and equations to a minimum, while retaining the essence of the physics that have the greatest impact on the radiative transfer model. The purpose of this paper is to describe a new radiative transfer model, unique in that it uses an iterative method to converge on a solution to the layered, two-flow radiative transfer equation with collimated irradiance. This method allows the modified (with a specular component) two-flow equations to be applied to a stratified water body modeled with any number of layers. This new model accounts for specular (collimated) irradiance below the water's surface and utilizes boundary conditions that allow the absorption, backscatter, beam attenuation, and conversion (from specular irradiance to diffuse irradiance) coefficients to vary as a function of depth These analytical solutions to the two-flow equations used in this research are an extension of those developed and advanced by Bostater and Lamb[3], Bostater, Ma et al[4], Bostater, Ma, and McNally[5] and modified to their present forms by Bostater and Huddleston[6] and Bostater, Huddleston, and Tepel[7].

2. METHODS

The analytical solution to the radiative transfer equation allows the simulation of the direct and indirect irradiant light fields according to the two-flow equations which are given by:

$$\frac{dE_d(z)}{dz} = -(a+b)E_d(z) + bE_u(z) + cE_s(z), \tag{2}$$

$$\frac{dE_u(z)}{dz} = (a+b)E_u(z) - bE_d(z) - cE_s(z), \tag{3}$$

$$\frac{dE_s(z)}{dz} = -\alpha E_s(z). \tag{4}$$

The analytical solution to the two-flow equations above, including a specular or collimated light component, for a homogeneous (non-layered) water body (here after referred to as the case IIa model) are described in Bostater et al.[4,5,6] and the derivation will not be repeated here, except to give the final equations:

$$E_d(z) = \frac{E_d(0) - m}{2}X + \frac{\beta_d(0) + \alpha m}{2\psi}Y + me^{-\alpha z}, \tag{5}$$

$$E_u(z) = \frac{E_u(h) - ne^{-\alpha h}}{2}V - \frac{\beta_u(h) + \alpha ne^{-\alpha h}}{2\psi} + ne^{-\alpha z}, \tag{6}$$

$$E_s(z) = E_s(0)e^{-\alpha z}. \tag{7}$$

where:

$$X = e^{\psi h} + e^{-\psi h}, \tag{8}$$

$$Y = e^{\psi h} - e^{-\psi h}, \tag{9}$$

$$m = \frac{-c(\alpha - a - 2b)}{\alpha^2 - \psi^2} E_s(0),$$ (10)

$$n = \frac{c(\alpha + a + 2b)}{\alpha^2 - \psi^2} E_s(0),$$ (11)

$$V = e^{\psi(z-h)} + e^{-\psi(z-h)},$$ (12)

$$W = e^{\psi(z-h)} - e^{-\psi(z-h)},$$ (13)

$$\beta_d(0) = -(a+b)E_d(0) + bE_u(0) + cE_s(0),$$ (14)

$$\beta_u(h) = (a+b)E_u(h) - bE_d(h) - cE_s(h),$$ (15)

And,

$$\psi = \sqrt{a^2 + 2ab}.$$ (16)

The solutions to the two-flow equations, including a specular light component, for a stratified or layered water body (here after referred to as the case IIb model) are described below. The case IIb model solutions are a generalization of the case IIa model solutions shown above (equations 5, 6, and 7) so that the water column does not have to be homogeneous, but can be a series of layers where the chemical properties within a particular layer are homogeneous, and each layer can have different chemical properties. Equation 5 can become more general by noting that $\beta_d(0)$ and "m" can also be written by adding an "i" for the layer number and using equations 10 and 14 to obtain:

$$\beta_d(0,i) = \frac{dE_d(0,i)}{dz(i)} =$$
$$-(a(i) + b(i))E_d(0,i) + b(i)E_u(0,i) + c(i)E_s(0,i),$$ (17)

and,

$$m(i) = \frac{-c(i)(\alpha(i) + a(i) + 2b(i))}{(\alpha(i))^2 - (\psi(i))^2} E_s(0,i).$$ (18)

The "i" designation is the i-th layer of a water column and "0" is depth z=0 for layer "i". Substituting equation 17 and 18 into equation 2 and rearranging, gives a general solution for $E_d(z,i)$:

$$E_d(z,i) = \frac{E_d(0,i) - m(i)}{2}\left(e^{\psi(i)z(i)} + e^{-\psi(i)z(i)}\right)$$

$$\left[\frac{-(a(i)+b(i))E_d(0,i)+b(i)E_u(0,i)+c(i)E_s(0,i)}{2\psi(i)}\right]$$

$$\times\left(e^{\psi(i)z(i)} - e^{-\psi(i)z(i)}\right) + m(i)e^{-\alpha(i)z(i)}$$

$$= \left[\frac{\psi(i)-a(i)-b(i)}{2\psi(i)}e^{\psi(i)z(i)} + \frac{\psi(i)+a(i)+b(i)}{2\psi(i)}e^{-\psi(i)z(i)}\right]E_d(0,i) \tag{19}$$

$$+\left[\frac{b(i)}{2\psi(i)}\left(e^{\psi(i)z(i)} - e^{-\psi(i)z(i)}\right)\right]E_u(0,i)$$

$$+\left[\frac{c(i)-m(i)\alpha(i)}{2\psi(i)}\left(e^{\psi(i)z(i)} - e^{-\psi(i)z(i)}\right) + 2\psi(i)e^{-\alpha(i)z(i)}\right]E_s(0,i)$$

The results of equation 19 give the downwelling vector irradiance at depth, "z", of layer "i". The downwelling irradiance at depth "z" of layer "i" $E_d(z,i)$ is set equal to the downwelling irradiance at the top of layer "i+1":

$E_d(z,i) = E_d(0,i+1)$ for energy conservation and the downwelling irradiance can be summed at discrete thicknesses over the total depth of the water column.

Using similar procedures, the general solution for upwelling vector irradiance for upwelling vector irradiance at depth, "0", of layer "i", is:

$$E_u(0,i) = \frac{E_u(z,i) - n(i)e^{-\psi(i)z(i)}}{2}\left(e^{\psi(i)z(i)} + e^{-\psi(i)z(i)}\right)$$

$$-\left[\frac{(a(i)+b(i))E_u(z,i)-b(i)E_d(z,i)-c(i)E_s(z,i)+\alpha(i)n(i)e^{-\alpha(i)z(i)}}{2\psi(i)}\right] \tag{20}$$

$$\times\left(e^{\psi(i)z(i)} - e^{-\psi(i)z(i)}\right) + n(i).$$

Substituting the layered version of equation 11:

$$n(i) = \frac{-c(i)(a(i)+2b(i)-\alpha(i))E_s(0,i)}{(\alpha(i))^2 - (\psi(i))^2}, \tag{21}$$

into equation 21 and rearranging, one obtains a general solution for $E_u(0,i)$:

$$E_u(0,i) = \left[\begin{array}{l} \dfrac{(\psi(i)+a(i)+b(i))}{2\psi(i)}e^{\psi(i)z(i)} + \\[3mm] \dfrac{(\psi(i)-a(i)-b(i))}{2\psi(i)}e^{-\psi(i)z(i)} \end{array}\right] E_u(z,i)$$

$$+ \left[\frac{b(i)}{2\psi(i)}\left(e^{\psi(i)z(i)} - e^{-\psi(i)z(i)}\right)\right] E_d(z,i) \tag{22}$$

$$+ \left[\frac{c(i)}{2\psi(i)}\left(e^{\psi(i)z(i)} - e^{-\psi(i)z(i)}\right)\right] E_s(z,i)$$

$$+ \left[\frac{n(i)}{2\psi(i)}\left(\begin{array}{l} 2\psi(i) - \psi(i)e^{-\psi(i)z(i)}\left(e^{\psi(i)z(i)} + e^{-\psi(i)z(i)}\right) \\[2mm] -\alpha(i)e^{-\psi(i)z(i)}\left(e^{\psi(i)z(i)} + e^{-\psi(i)z(i)}\right) \end{array}\right)\right] E_s(0,i)$$

The results of equation (22) give the upwelling vector irradiance at depth, "0", of layer "i". The upwelling irradiance at depth "0" of layer "i" $E_u(0,i)$ is set equal to the upwelling irradiance at the bottom of layer "i-1":

$E_u(0,i) = E_u(z,i-1)$, where "z" is the thickness of layer "i". The upwelling irradiance is summed at discrete thicknesses over the total depth of the water column to find the total upwelling vector irradiance at the water surface.

3. OVERVIEW OF THE ITERATIVE, LAYERED TWO-FLOW MODEL

For a layered water column or layered media, the two-flow equations cannot be solved by using the Cauchy boundary conditions employed by Bostater et al [4,5]. This is because the upwelling irradiance at the bottom of each layer is not known until the downwelling diffuse and direct irradiance reaches the bottom (h) of the water column. This limitation can be overcome by solving the two-flow equations iteratively.

The amount of downwelling light backscattered in each layer, the amount of upwelling light backscattered in each layer, and the amount of collimated light that is converted to diffuse light are independently calculated. In order to calculate the downwelling irradiance at the next layer interface, the downwelling irradiance in the top of the layer is added to the amount of upwelling light backscattered into this layer and the amount of collimated light converted to diffuse downwelling light in this layer. The upwelling light in each layer is determined in the same manner.

In the first iteration, the upwelling light backscattered into each layer is set to zero. The iterative procedure is repeated using the most recently calculated values of the backscattered and converted light until successive values of the upwelling light at the surface converge, or agree to within a specified tolerance (ε) of $\varepsilon \le 10^{-10}$. Figure 1 shows a schematic of the iterative method for solving the layered two-flow equations.

In this research, convergence is defined as when the difference in $E_u(0)$ between successive iterations is less than 1×10^{-10} Wm^{-2}. This factor is smaller than typical irradiance meters can measure. For all model test cases (60 cases total), the maximum number of iterations to converge is 7. The minimum number of iterations to converge is 2. The model requires more iterations to converge in the red portion of the wavelength spectrum when both chlorophyll-a and suspended materials concentrations are high.

The choice of the proper values of the layer thickness is of considerable importance in the iterative two-flow (case IIb) model. In deciding upon the proper layer thickness, a decision as to the desired accuracy must be made. A check upon the accuracy of the current model is shown in the comparison of the case IIb model results with the case IIa model results. Selecting the layer thickness that minimized the absolute value of the difference between the subsurface irradiance reflectance values of the case IIa and case IIb models determined the proper layer thickness. After considerable experimentation with various layer thicknesses, the optimum layer thickness, as a function of chlorophyll-a and suspended materials concentrations, is outlined in Figure 2.

There are instances when attempting to produce a family of reflectance signatures in order to discern a hinge point, that it best to use the same layer thickness for each reflectance signature rather than using the optimum thickness as described by Figure 2. It is best to use the same layer thickness for each reflectance signature when the component concentration varied is suspended sediments and chlorophyll-a concentration is greater than zero. Otherwise, the influence of the thickness variation on the shape of the reflectance signatures due to rounding error will preclude the production of a single hinge point.
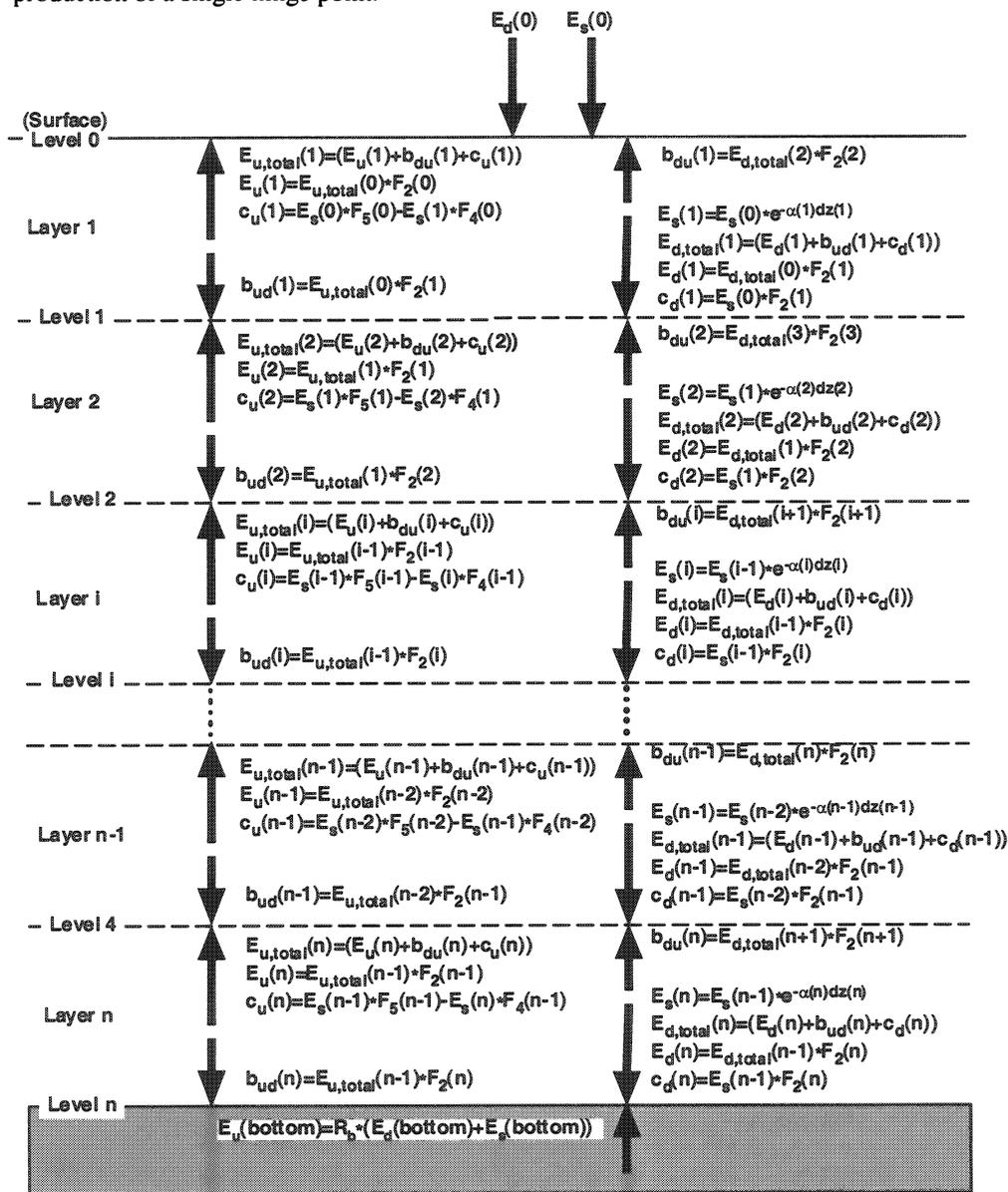
Figure 1. Schematic of the iterative case IIb model calculation process for each layer in the water column.
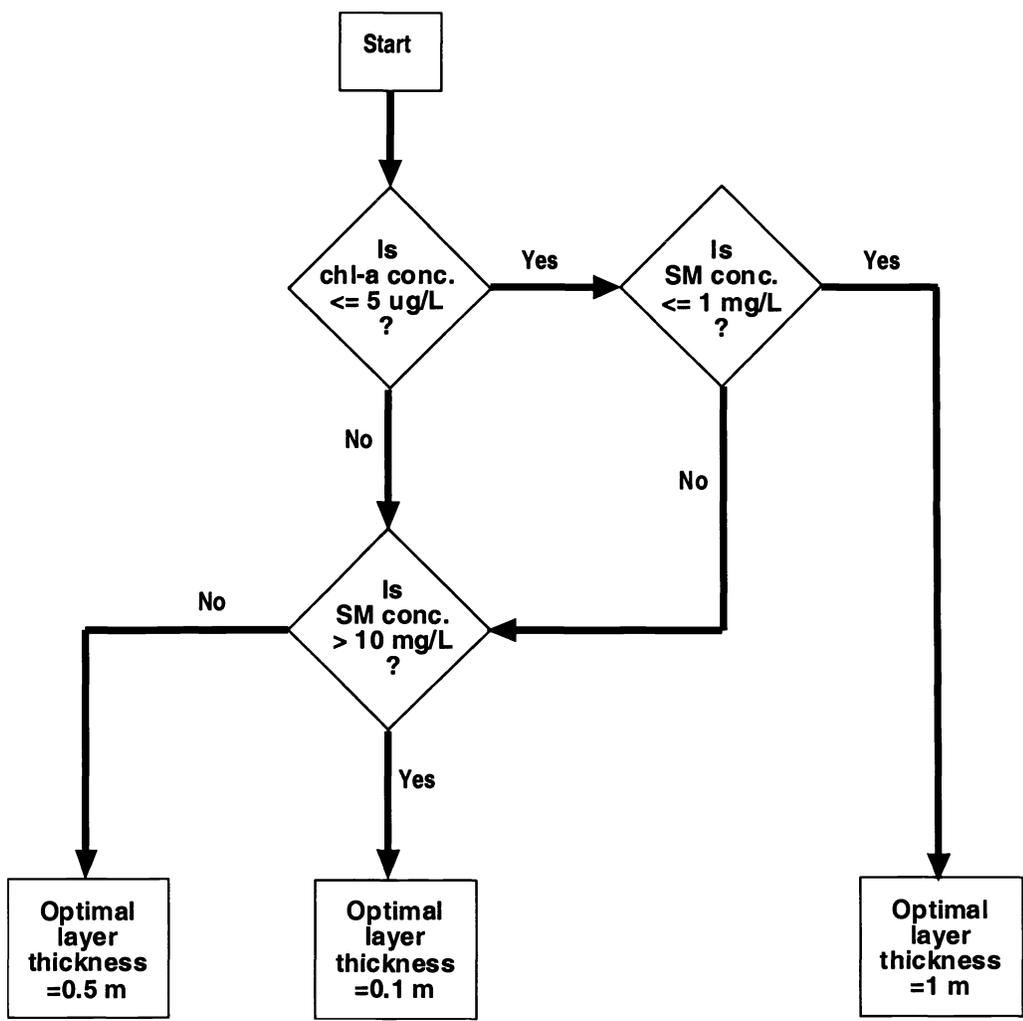
Figure 2. Flow diagram of the optimal layer thickness choice for the iterative case IIb model as a function of chlorophyll-a and suspended materials concentrations.

4. RESULTS

Subsurface irradiance reflectance signatures for a natural water column were calculated for both the homogeneous and the layered two-flow models by using specific absorption coefficients and estimated specific backscattering coefficients for constituents in the water using coefficients and data collected from the Banana River and coastal Atlantic Ocean by Bostater and Gimond[8]. The common input parameters for the model runs were: (1) the conversion coefficient, "c", was determined empirically to be 2.85 times the backscattering coefficient "b"; (2) the zenith angle (θ_z) was assumed to be 20°; (3) the bottom type was assumed to be comprised of sea grass; (4) the wind speed was assumed to be 6 m/s.

Figures 3 and 4 shows the subsurface irradiance reflectance signatures for various chlorophyll-concentrations (0-20 $\mu g / L$), while the suspended material and dissolved organic carbon concentrations were held to zero. Figures 3 and 4 include the worst case comparison in terms of the mean percent error and root mean square error. The case IIb layered model (Figure 4) was run for a layer thickness of 1 m. In the 400 to 600 nm range, the case IIb model over estimates subsurface irradiance reflectance as compared to the homogeneous (case IIa) model for chlorophyll-a concentrations less than or equal to 1 $\mu g / L$. The case IIb model underestimates subsurface irradiance reflectance in the 400 to 600 nm range for chlorophyll-a concentrations greater than 1 $\mu g / L$. Note also that the case IIb model shifts the hinge point to the right (approximately 490 nm) as opposed to the case IIa model (Figure 3) where the hinge point is at approximately 460 nm.
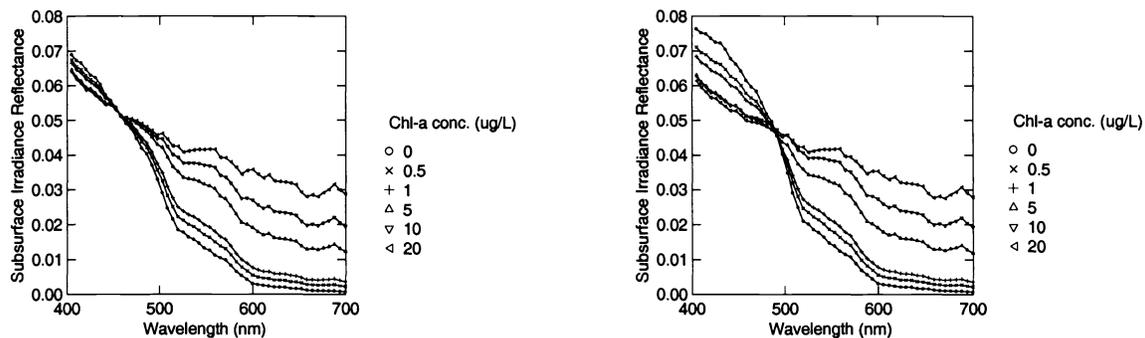

Figure 3 (left). Subsurface irradiance reflectance signatures Rw (0) calculated using the Case IIa (homogeneous) model for various chlorophyll-a concentrations (0-20 $\mu g / L$) in natural water. The concentrations of suspended material and dissolved organic carbon were held at zero. The depth of the water column for this model run was 50 m with an assumed sea grass type bottom. The wind speed was 6 m/s.

Figure 4 (right). Subsurface irradiance reflectance signatures $R_w(0)$ calculated using the Case IIb (layered) model, with a layer thickness of 1 m, for various chlorophyll-a concentrations (0-20 $\mu g / L$) in natural water. The concentrations of suspended material and dissolved organic carbon were held at zero. The depth of the water column for this model run was 50 m with an assumed sea grass type bottom. The wind speed was 6 m/s.

Figures 5 and 6 show the subsurface irradiance reflectance signatures for various suspended materials concentrations (0-20 mgC/L). Figures 5 and 6 include the best case comparison in terms of the mean percent error and root mean square error. The concentration of chlorophyll-a was set to zero while dissolved organic carbon concentration was held to be 3 mgC/L. The reflectance signatures in Figure 6 were produced using the optimum thickness as described by Figure 2. For suspended materials concentrations of 0 to 1 mg/L, the thickness used was 1.0 m. For a suspended materials concentration of 5 mg/L, the thickness used was 0.5 m, and for suspended materials concentrations of 10 to 20 mg/L, the thickness used was 0.1 m. For suspended materials concentrations of 0 to 1 mg/L, the case IIb layered model over estimates subsurface irradiance reflectance for all wavelengths (400 to 700 nm) as compared to the case IIa homogeneous model. For a suspended materials concentration of 5 mg/L, the case IIb model under estimates subsurface irradiance reflectance for the wavelength range of 400 to 510 nm, and over estimates subsurface irradiance reflectance for the wavelength range of 510 to 700 nm. For suspended materials concentrations of 10 to 20 mg/L, the case IIb model over estimates subsurface irradiance reflectance, compared to the case IIa model, over the entire 400 to 700 nm range.
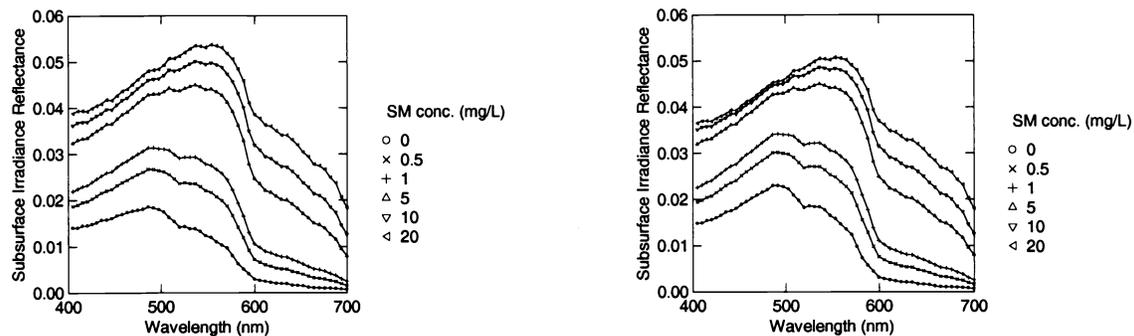
Figure 5 (left). Subsurface irradiance reflectance signatures $R_w(0)$ calculated using the Case IIa (homogeneous) model for various suspended material concentrations (0-20 mg/L) in natural water. The concentration of chlorophyll-a was set to zero and dissolved organic carbon was held at 3 mgC/L. The depth of the water column for this model run was 20 m with an assumed sea grass type bottom. The wind speed was 6 m/s.

Figure 6 (right). Subsurface irradiance reflectance signatures $R_w(0)$ calculated using the Case IIb (layered) model, with a layer thickness of 1 m, for suspended material concentrations of 0-1 mg/L with a layer thickness of 0.5 m for suspended material concentrations of 5 and 10 mg/L, and with a layer thickness of 0.1 m for a suspended material concentration of 20 mg/L, in natural water. The concentration chlorophyll-a was set to zero and dissolved organic carbon was held at 3 mgC/L. The depth of the water column for this model run was 20 m with an assumed sea grass type bottom. The wind speed was 6 m/s.

Figure 7 shows the comparison of the subsurface irradiance reflectance as calculated by the case IIa homogeneous model and the case IIb layered model for the worst case in terms of the percent mean error and the root mean square error. These particular reflectance signatures are from Figures 3 and 4 where the chlorophyll-a concentration was zero. In this instance, the mean percent error was 10.14% and the percent root mean square error was 0.44%. Figure 8 shows the comparison between the two models for the best case in terms of percent mean error and the root mean square error. These reflectance signatures are from Figures 5 and 6 where the suspended sediments concentration was 5 mg/L. In this instance, the mean percent error was 0.74%, the root mean square error was 0.01%.
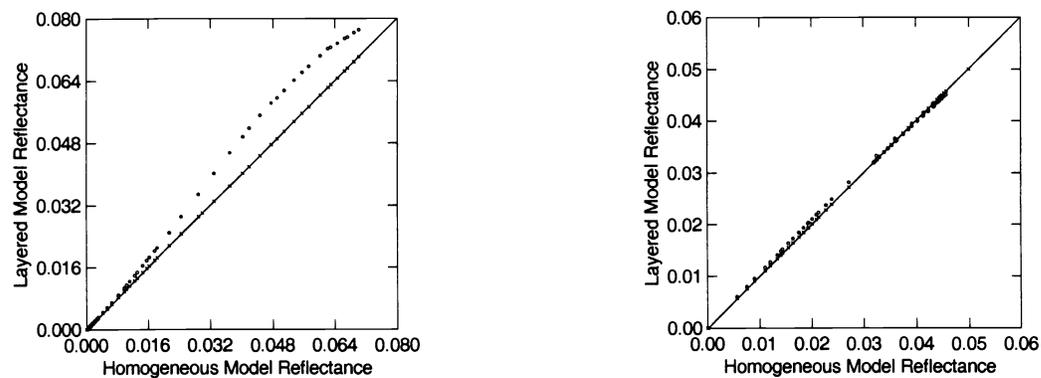

Figure 7 (left). Comparison between the Case IIa analytical, homogeneous water column model and the Case IIb, analytical, layered water column model with layer thickness equal to 1.0 m and Chl-a conc. = 0 μg/L, DOC conc. = 0 mgC/L, and SM conc. = 0 mg/L, depth = 50m, and a sea grass bottom type.

Figure 8 (right). Comparison between the Case IIa analytical, homogeneous water column model and the Case IIb, analytical, layered water column model with layer thickness equal to 0.5 m and Chl-a conc. = 0 μg/L, DOC conc. = 3 mgC/L, and SM conc. = 5 mg/L, depth = 20m, and a sea grass bottom type.

The results of the case IIb layered model with varying water column components and with the insertion of various target layers are shown. In the model runs below, the atmospheric parameters and the absorption, backscattering, and conversion coefficients were as described above. The absorption, backscattering, and conversion coefficients were held constant in each layer and were assumed to be the same in both the upwelling and downwelling directions.

Figures 9, 10 and 11 demonstrate how the water surface reflectance signatures change by the insertion of a "target" layer at various depths in the water column. Figure 9 shows a "target" layer (10 m thick) containing 6 µg/L chlorophyll-a, 18 mgC/L dissolved organic carbon, and 18 mg/L suspended material at various depths in a column of pure sea water (0 µg/L chlorophyll-a, 0 mgC/L dissolved organic carbon, and 0 mg/L suspended material). The total water column depth was 50 m. Note that the wavelength bands at approximately 430 nm and 540 nm would be the optimum bands to discriminate the depth of the "target" layer for the shown scenarios.
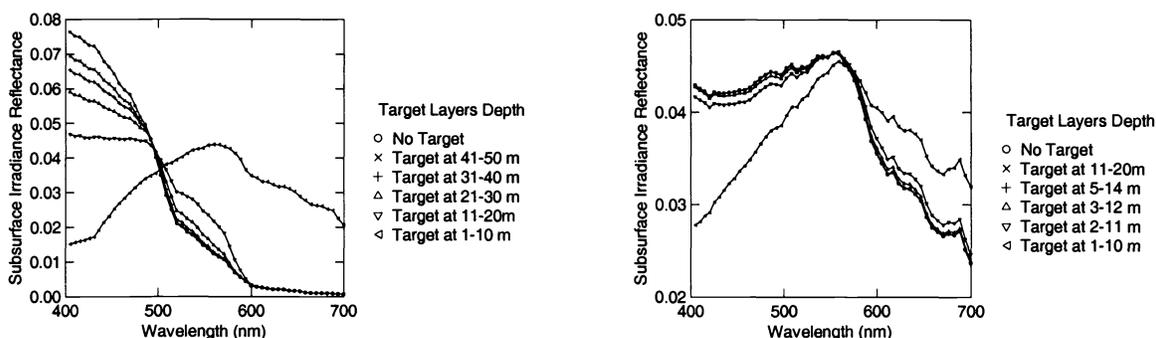

Figure9 (left). Layered model results indicating the influence of a unique water quality layer on the synthetic water surface reflectance. The background water column concentrations were set at 0 µg/L chl-a, 0 mgC/L DOC, and 0 mg/L suspended material (SM), and a sea grass bottom reflectance. The unique layers or "target layers" with unique water quality concentrations were placed at various depths as indicated. "Target layers" had water column concentrations of 6 µg/L chl-a, 18 mgC/L DOC, and 18 mg/L suspended material (SM). Layered model was run for a 50 m water column depth.

Figure 10 (right). Layered model results indicating the influence of a unique water quality layer on the synthetic water surface reflectance. The background water column concentrations were set at 12 µg/L chl-a, 3 mgC/L DOC, and 7 mg/L SM, and a sea grass bottom reflectance. The unique layers or "target layers" with unique water quality concentrations were placed at various depths as indicated. "Target layers" had water column concentrations of 26 µg/L chl-a, 20 mgC/L DOC, and 18 mg/L suspended material (SM). Layered model was run for a 20 m water column depth.

Figure 10 shows a "target" layer (10 m thick) containing 26 µg/L chlorophyll-a, 20 mgC/L dissolved organic carbon, and 18 mg/L suspended material at various depths in a column of water. The total water column depth was 20 m. The background water column concentrations were 12 µg/L chlorophyll-a, 3 mgC/L dissolved organic carbon, and 7 mg/L suspended material). The "target" layers in the more turbid waters of the simulations in Figure 10 can not be discerned at as great a depth as in clear sea water background simulations shown in Figure 9. For the scenarios in Figure 10, the wavelength bands at approximately 470 nm and 630 nm would be the optimum bands to discriminate the depth of the "target" layer.

Figure 11 is similar to Figure 10 except that a coral "target" layer (1 m thick) was inserted at various depths in a column of pure sea water (0 µg/L chlorophyll-a, 0 mgC/L dissolved organic carbon, and 0 mg/L suspended material). The total water column depth was 10 m. The wavelength bands at approximately 430 nm and 575 nm would be the optimum bands to discriminate the depth of the coral "target" layer.

Figure 12 shows the influence on water surface reflectance signatures by the insertion of a "target" layer (1 m thick) at the bottom of the water column and then changing the water column depth. A "target" layer with concentrations of 3 µg/L chlorophyll-a, 3 mgC/L dissolved organic carbon, and 36 mg/L suspended material was inserted at the bottom of a column of pure sea water (0 µg/L chlorophyll-a, 0 mgC/L dissolved organic carbon, and 0 mg/L suspended material). The total water column depth, starting at 20 m and ending at 1m, was decreased as indicated in Figure 12. The wavelength bands at approximately 430 nm and 575 nm would again be the optimum bands to discriminate the depth of the "target" layer. The vertical concentrations of the water quality variables shown in Figure 13 are the basis of the synthetic water surface reflectance signatures shown in Figure 14. The lack of chlorophyll-a (Profile No. 3 of Figure 13) showed the greatest impact on the synthetic water surface reflectance signatures. The optimum wavelength band for discriminating between the different profiles of the water quality variables would be at approximately 575 nm.
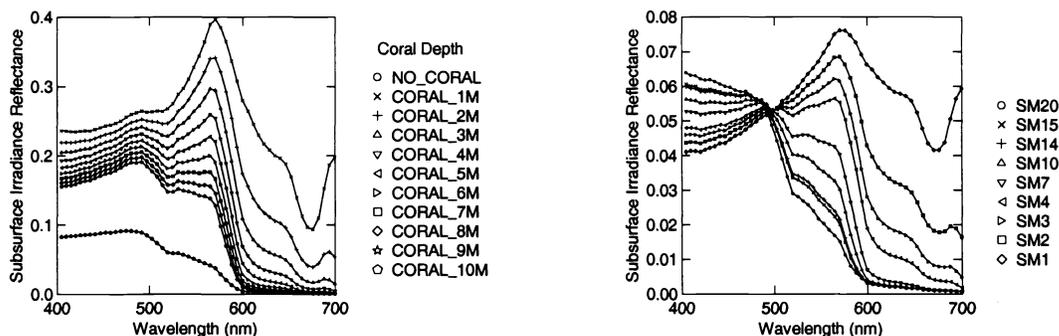

Figure 11 (left). Layered model results indicating the synthetic water surface reflectance simulated by inserting a coral layer "target" at varying depths (in meters) as indicated. The water column was a constant depth of 10 m. Homogeneous water column concentrations were set at 0 µg/L chl-a, 0 mgC/L DOC, and 0 mg/L suspended material (SM), with a sand bottom type.

Figure 12 (right). Layered model results indicating the influence of a unique water quality layer on the synthetic water surface reflectance. The background water column concentrations were set at 0 µg/L chl-a, 0 mgC/L DOC, and 0 mg/L SM, and a sea grass bottom reflectance. The unique layers or "target layers" with unique water quality concentrations were placed at the bottom (one meter thickness) of the water column and the water column depth was decreased as indicated. "Target layers" had water column concentrations of 3 µg/L chl-a, 3 mgC/L DOC, and 36 mg/L suspended material (SM).

5.DISCUSSION

The layered two-flow model results suggest that the nonhomogeneous characteristics of the water column and "targets" within the water column influence the calculated surface reflectance and thus would affect measured satellite or aircraft based sensor reflectance, associated imagery and related algorithms. The layered (case IIb) model agrees to within ±0.44% (RMS) error of the homogeneous (case IIa) model for the test case comparisons.

The model in its present form may be improved by overcoming some of the model limitations as follows: Generally, the case IIb layered two-flow model under estimates the subsurface irradiance reflectance when compared to the case IIa homogeneous model if the chlorophyll-a concentration is high (≥ 10 µg/L). If the chlorophyll-a concentration is low (≤ 1 µg/L), the case IIb model over estimates subsurface irradiance reflectance when compared to the case IIa homogeneous model. This is due to the computational rounding error that occurs at each layer interface of the case IIb model. More is needed to determine an optimal numerical technique to minimize this rounding error.
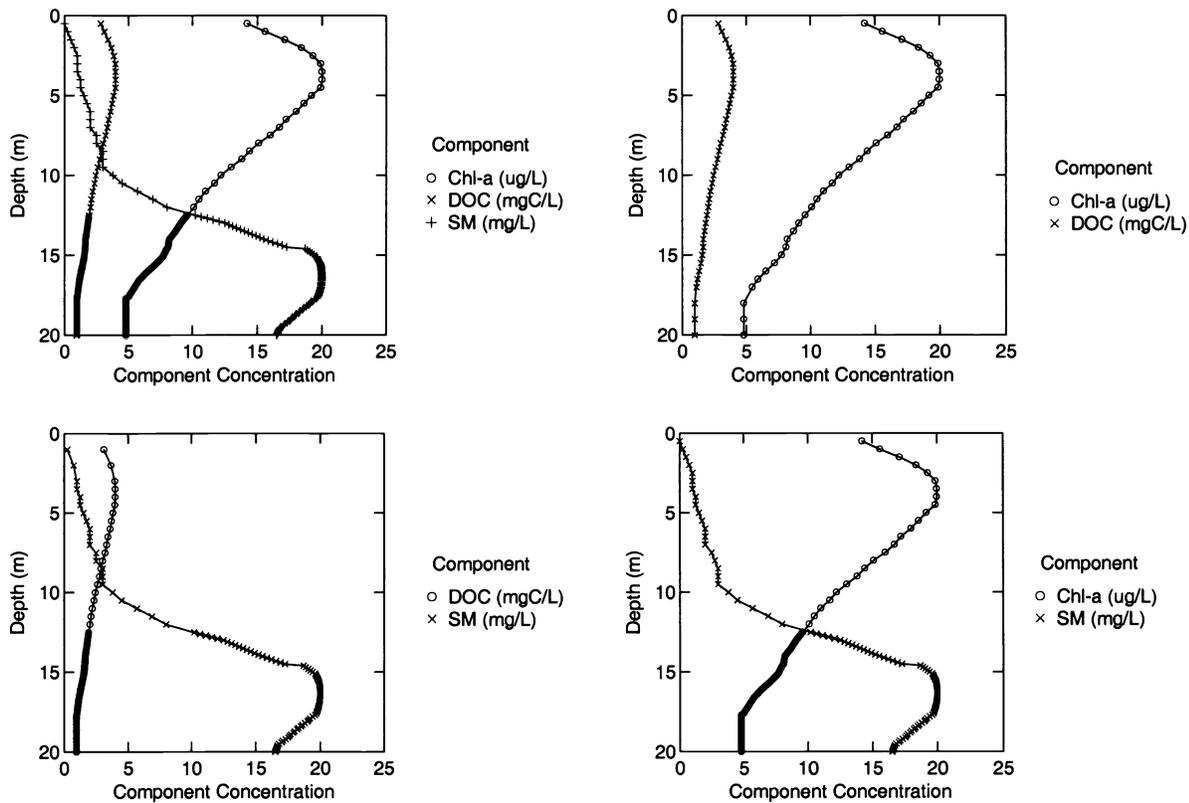
Figure 13. Assumed vertical concentrations of water quality variables for the four reflectance signatures shown below. The reflectance signatures in Figure 14 correspond to the vertical profiles above as follows: Top, left hand figure is "Profile No. 1". Top, right hand figure is "Profile No. 2". Bottom, left hand figure is "Profile No. 3". Bottom, right hand figure is "Profile No. 4".
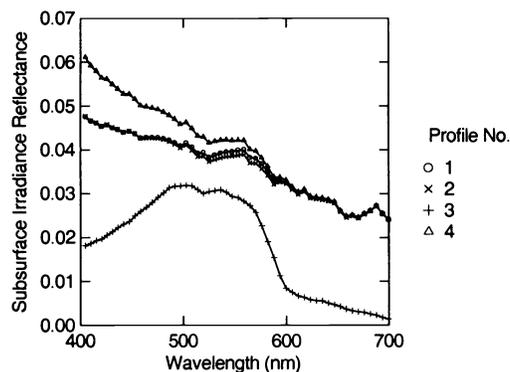

Figure 14. Layered model results indicating the synthetic subsurface irradiance reflectance simulated as a function of varying the vertical profiles of chlorophyll-a (Chl-a), dissolved organic carbon (DOC), and suspended material (SM) as indicated in Figure 2 for a 20 m water column depth and a sand and silt bottom type.

The atmospheric remote sensing model does not take into account clouds in the atmosphere and is valid only if one assumes a cloudless sky.

The assumption that the absorption, backscatter and conversion coefficients are the same in both the upwelling and downwelling directions is not true for most water types due to the shape factors (r_d and r_u) for upwelling and downwelling light[9,10,11]. More work needs to be implemented to properly define these specific coefficients and to ensure their generality to a region of interest. It will be beneficial to continue development of Monte Carlo model[12,13] to determine the values of the mean cosines (μ_d and μ_u) and the shape factors (r_d and r_u) for upwelling and downwelling light in various water types.

Finally, a comprehensive scale analysis involving the various factors (i.e. concentrations; layer thicknesses; sun angles; wind conditions; etc.) applied to the layered (case IIb) model solution, could produce simplified equations thereby making inversion possible.

ACKNOWLEDGMENTS

REFERENCES

1. Perovich, D. K. (1989). A two-stream multiplayer, spectral radiative transfer model for sea ice, U.S. Army Cold Regions Research and Engineering Laboratory, 20 pp.
2. Preisendorfer, R., 1978, *Hydrologic Optics*, Vol. I-VI, NOAA/ERL, Honolulu, HI, pp. 1757, 1978.
3. Bostater, C. and A. Lamb, "Innovative use of in-situ and airborne measurements of electromagnetic radiation in near shore environments," In: *Proc. 2nd Intl. Conference on Spectral Remote Sensing Research*, San Diego, CA, USACOE, July 1994, pp. 673-682.
4. Bostater, C., W. Ma, T. McNally, M. Gimond, and A. P. Lamb, "Application of an optical remote sensing model," In: *Proceedings of the European Optical Society and SPIE – The International Society for Optical Engineering (EUROPTO), The European Symposium on Satellite Remote Sensing*, Paris, France, 25-28 September, 1995, Volume 2586, pp. 32-43.
5. Bostater, C., W. Ma, and T. McNally, "Advancement of an optical remote sensing model to simulate the underwater light field", In: *Proceedings of the European Optical Society and SPIE – The International Society for Optical Engineering (EUROPTO), The European Symposium on Satellite Remote Sensing III*, Taormina, Italy, 23-27 September, 1996, Volume 2959, pp. 180-189.
6. Bostater, C., and L. Huddleston, "Layered analytical radiative transfer model for simulating water color of coastal waters and algorithm development," In: *Proceedings of the European Optical Society and SPIE – The International Society for Optical Engineering (EUROPTO), Remote Sensing of the Ocean and Sea Ice 2000*, Barcelona, Spain, 28-29 September, 2000, Volume 4172, pp. 153-161.
7. Bostater, C., L. Huddleston, and M. Tepel, "Improvements to a layered analytical irradiance model for application to coastal waters with depth dependent water constituents, various bottom types, and variable water depths," In: *Proceedings of the European Optical Society and SPIE – The International Society for Optical Engineering (EUROPTO), Remote Sensing of the Ocean and Sea Ice 2001*, Toulouse, France, 18 and 20-21 September, 2001, Volume 4544, pp. 236-245.
8. Bostater, C. and M. Gimond, "Using aircraft based high resolution reflectance signatures and specific absorption coefficients to remotely estimate coastal water quality," In: *Proc. 2nd Intl Airborne Remote Sensing Conference and Exhibition*, San Francisco, California, 1996.
9. Aas, E., "Two-stream irradiance model for deep water," *Applied Optics* 26(11), pp. 2095-2101, 1987.
10. Stavn, R. H. and A. D. Weidemann, "Shape factors, two-flow models, and the problem of irradiance inversion in estimating optical parameters," *Limnology and Oceanography* 34(8), pp. 1426-1441, 1989.
11. Mobley, C. D., *Light in Water. Radiative Transfer in Natural Waters*, 592 pp., Academic Press, San Diego, 1994.

12. Bostater C., M. Gimond, and M. Campbell, "Comparing a hyperspectral Monte-Carlo approach for simulating water surface reflectance signatures based upon radiative transfer theory: simulating clear water and Caribbean Sea bottom types," In: *Proceedings of the European Optical Society and SPIE – The International Society for Optical Engineering (EUROPTO), Remote Sensing of the Ocean and Sea Ice 2000*, Barcelona, Spain, 28-29 September, 2000, Volume 4172, pp. 199-208.
13. Bostater, C. and M. Gimond, "Comparison between an analytical and Monte Carlo hyperspectral reflectance model for coastal remote sensing," In: *Proceedings of the European Optical Society and SPIE – The International Society for Optical Engineering (EUROPTO), Remote Sensing of the Ocean and Sea Ice 2001*, Toulouse, France, 18 and 20-21 September, 2001, Volume 4544, pp. 108-122.